Des Nombres et des Mondes (E. Benoît, J-Ph. Furter eds),
Hermann, Paris, 2013, 99-118.

Towards a nonstandard model for neurogeometry*

Jean Petitot†

Abstract

We present what we call a "neurogeometrical" model of the first primary visual area V1. We explain how nonstandard analysis can be used in order to solve one of the difficulties of such a model.

A Guy Wallet

1 Introduction

What I call "neurogeometry" concerns the geometrical models of the functional architectures of the brain, that is of the connectivity of its different area. These functional architectures explain how the activation of the areas can be equivalent to well defined computations such as contour extraction. I will focus here on the functional architecture of the first primary visual cortical area V1, present a neurogeometrical model for it and propose some remarks on the relevance of a nonstandard approach of this model.

I will present first some neurophysiological data, then introduce the geometrical model and finally explain how nonstandard analysis can be used in order to solve one of the difficulties of such a model.

*Guy Wallet Conference "Des Nombres et des Mondes", La Rochelle, June 2011.

†CAMS (École des Hautes Études en Sciences Sociales), Paris, France.
e-mail : jean.petitot@polytechnique.edu
URL : http://jean.petitot.pagesperso-orange.fr/

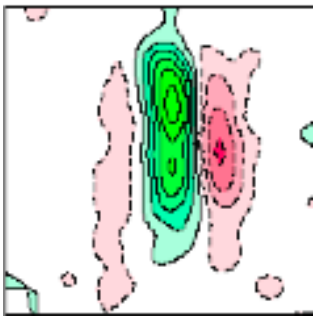

Figure 1: The level curves of a typical receptive profile of a simple neuron of visual area V1.

2 Neurons as filters

In the linear approximation, "simple" neurons of the first visual cortical area V1 operate as filters on the optical signal coming from the retina. Their receptive fields (RF), that is the bundle of photoreceptors they are connected with via the retino-geniculo-cortical pathways, have receptive profiles (a transfert function in the sense of signal analysis) with a characteristic shape: they are highly anisotropic and oriented along a preferential orientation.

Using sophisticated experimental methods, the level curves of these RFs can be recorded (see figure 1).

RPs operate by convolution on the signal $I(x, y)$, (x, y) being coordinates on the retina R, (see Petitot [15] and [16]). They implement a wavelet analysis and can be modeled either by second order derivatives of Gaussians $G = \exp(-(x^2 + y^2))$ (which are typical examples of wavelets), or by the real part of Gabor wavelets $\varphi(x, y) = \exp(i2x)\exp(-(x^2 + y^2))$ (see figure 2).

Specialists such as Richard Young *et al.* [23] devoted many studies to find the best models, and opted for the Gaussian ones. Since $DG * I = D(G * I)$ for any differential operator D,

> "The initial stage of processing of receptive fields in the visual cortex approximates a 'derivative analyzer' that is capable of estimating the local spatial and temporal directional derivatives of the intensity profile in the visual environment."

3 The functional architecture of area V1

3.1 Hypercolumns

Due to the specific shape of their RP, the simple cells of V1 measure, at a certain scale, pairs (a, p) of a spatial (retinal) position $a = (x, y)$ and

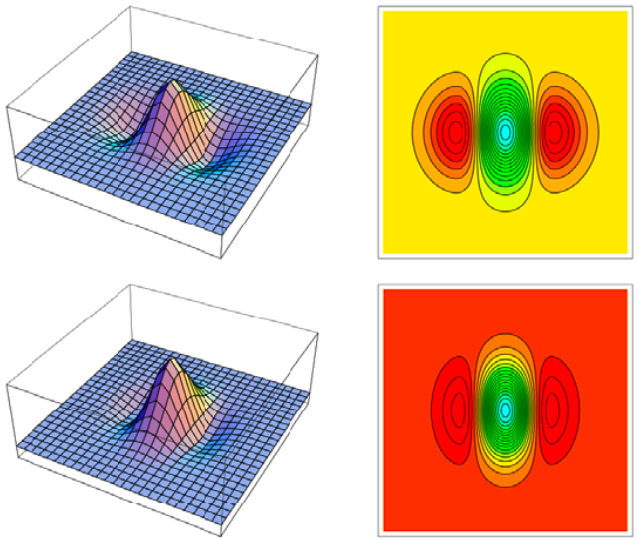

Figure 2: Two models for the receptive profile of a V1 neuron: a second derivative of Gaussian $\varphi(x,y) = \frac{\partial^2 G}{\partial x^2}$ with $G = \exp\left(-\left(x^2+y^2\right)\right)$, and a Gabor function $\psi(x,y) = \exp(i2x)\exp\left(-\left(x^2+y^2\right)\right)$ (real part).

of a local orientation p at a. Such pairs (a,p) are called *contact elements* in differential geometry.

A fundamental experimental fact, discovered by the Nobel Prizes Hubel and Wiesel, is that, for a given position $a = (x,y)$ in the retinal plane R, the simple neurons with variable orientations p constitute an *anatomically* definable micromodule called an "hypercolumn". So the hypercolumns associate *retinotopically* to each position a of the retinal plane R a full exemplar P_a of the space P of orientations p at a (P can be modeled either by the projective line $\mathbb{P}^1$, or by the unit circle $\mathbb{S}^1$, or by the real line $\mathbb{R}$). (See figure 3).

So, this part of the functional architecture of V1 implements the fibration $\pi : R \times P \to R$ with base R, fiber P, and total space $V = R \times P$. This is mathematically trivial, but by no means neurologically trivial since a neural implementation means that an *abstract* structure results phylogenetically *wired* in the material neural hardware.

The geometrical concept of a fibration formalizes Hubel's concept of "engrafting secundary variable" on the basic retinal variables (x,y):

> "What the cortex does is map not just two but many variables on its two-dimensional surface. It does so by selecting as the basic parameters the two variables that specify the visual field coordinates (...), and on this map it engrafts

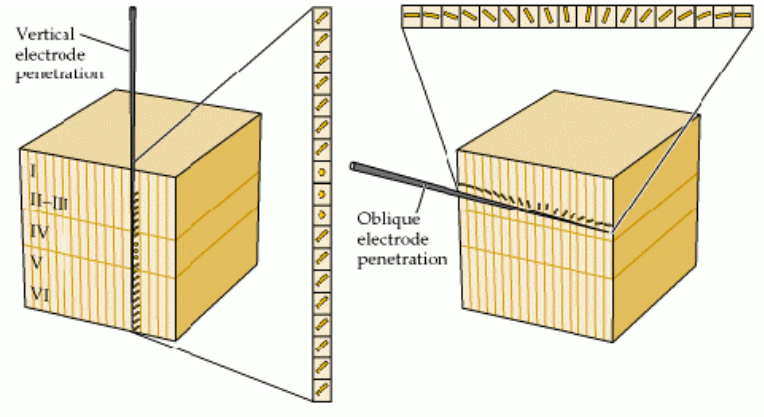

Figure 3: Hubel's and Wiesel's hypercolumns. Along a "vertical" penetration of the electrode into the cortical layers, the position and the orientation selected by the neurons are essentially constant. But along an "horizontal" penetration inside a single layer, the position remains approximately constant while the orientations rotate continuously.

> other variables, such as orientation and eye preference, by finer subdivisions." (Hubel [8])

3.2 Pinwheels

The abstract fibration $\pi : R \times P \to R$ is of dimension 3 but is implemented in neural layers of dimension 2. There exists therefore a *dimensional collapse*, which is empirically manifested by the fact that hypercolumns are geometrically organized in *pinwheels*. The cortical layer is reticulated by a lattice L of singular points which are the centers of the pinwheels and, locally around these singular points, all the orientations are represented by the rays of a "wheel", and these local wheels are glued together into a global structure.

The method, introduced by Bonhöffer and Grinvald in the early 1990s, of in vivo optical imaging based on activity-dependent intrinsic signals allows to acquire images of the activity of the superficial cortical layers and to visualize the pinwheels. Gratings with high contrast are presented many times (20-80) with, e.g., a width of 6.25° for the dark strips and of 1.25° for the light ones, at a velocity of $22.5°/s$, and along 8 different orientations. A window is opened in the skull above V1 and the cortex is illuminated with orange light. This is an efficient protocol because the concentration of deoxyhemoglobin increases when neurons are activated and the absorption spectrum of deoxyhemoglobin is maximal for wave lengths about 600 nm. The recorded images are then analyzed very carefully. One does the summation of the images of V1's activity

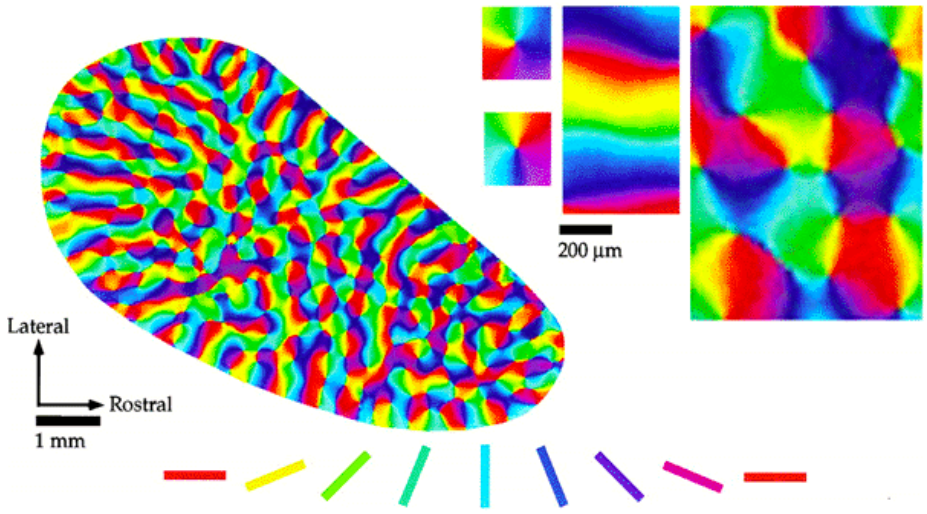

Figure 4: The pinwheel structure of tree shrew's V1. (From Bosking *et al.*[3]).

for the different gratings and constructs differential maps (differences between orthogonal gratings). The low frequency noise is eliminated and the maps are normalized by dividing the deviation relative to the mean value at each pixel by the global mean deviation.

In the following figure (4) due to William Bosking *et al.* [3] (David Fitzpatrick's group, Department of Neurobiology at Duke University) the orientations are coded by colors and iso-orientation lines are therefore coded by monocolor lines.

One observes essentially 3 classes of points:

1. regular points where the orientation field is locally trivial;
2. singular points near the center of the pinwheels;
3. saddle-points localized near the centers of the domains defined by the lattice of pinwheels.

Two adjacent singular points are of opposed chirality (clockwise and counterclockwise) and the direction field is like a field generated by topological charges with field lines connecting charges of opposite sign.

In the following figure (5) due to Shmuel and Grinvald [20] (cat's area 17, the equivalent of V1), the orientations are coded by colors but are also represented by small white segments. One can observe very well the two types of generic singularities of 1D foliations in the plane. They arise from the fact that, in general, the direction θ in V1 of a ray of a pinwheel is not the orientation p_θ associated with it in the visual field.

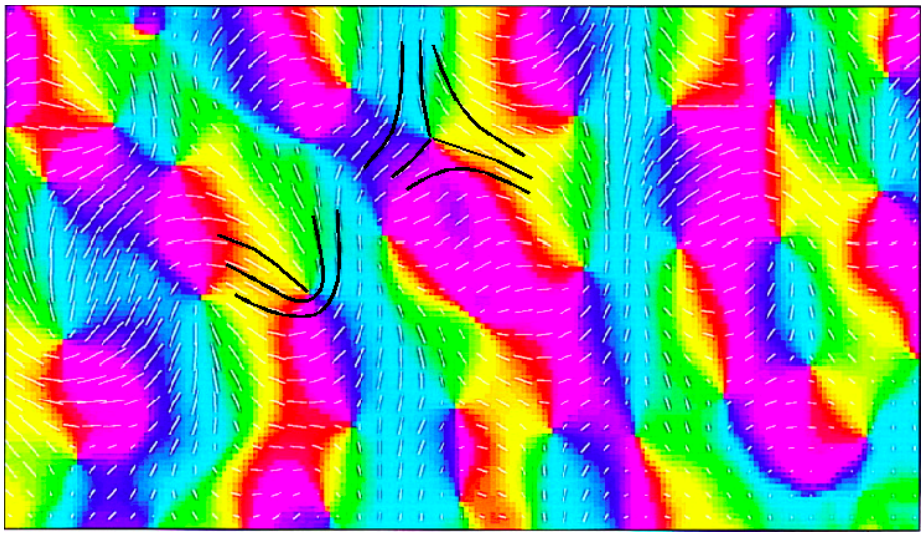

Figure 5: The field of orientations in V1 with its two types of singularities: end points and triple points. (From Shmuel and Grinvald [20]).

Indeed, when the ray rotates around the singular point with an angle φ the associated orientation rotates with an angle $\varphi/2$ and two diametrally opposed rays correspond therefore to orthogonal orientations. Pinwheels implement in fact a spin structure.

There are two cases. If the orientation p_θ associated with the ray of angle θ is $p_\theta = \alpha + \theta/2$ (with $p_0 = \alpha$), the two orientations will be the same for $p_\theta = \alpha + \theta/2 = \theta$, that is for $\theta = 2\alpha$. As α is defined modulo π, there exists only one solution and the singularity is an *end point*.

If the orientation p_θ associated with the ray of angle θ is $p_\theta = \alpha - \theta/2$, the two orientations will be the same for $p_\theta = \alpha - \theta/2 = \theta$, that is for $\theta = 2\alpha/3$. As α is defined modulo π, there exist three solutions and the singularity is a *triple point*.

Such models have been anticipated before in vivo optical imaging, in particular by Braitenberg soon after Hubel's and Wiesel's discovery of orientation hypercolumns (see, e.g., Baxter, Dow [2]).

3.3 Micro-structure near pinwheel centers

It is important to have some information on the V1 structure near pinwheel singularities. Pedro Maldonado *et al.* [11] have analyzed the fine-grained structure of orientation maps at the singularities. They found that

> "orientation columns contain sharply tuned neurons of different orientation preference lying in close proximity".

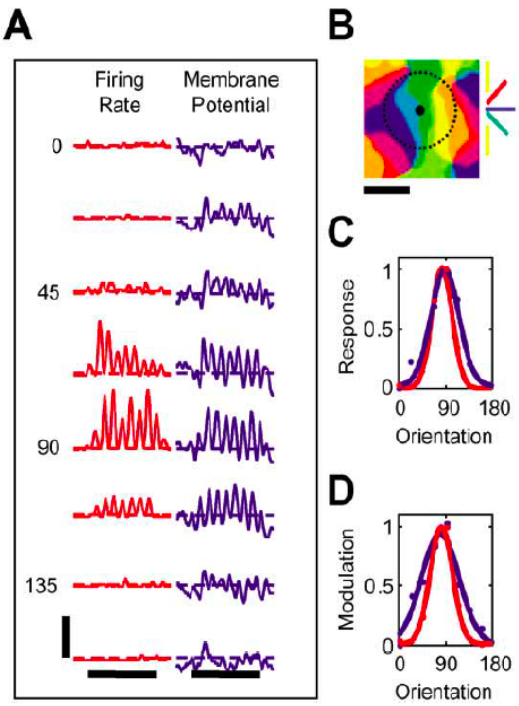

Figure 6: The response of a cell far for from a pinwheel center: spike response and membrane depolarization are both selective to orientation. Scales: 8 spikes/s, 10mV, 2s. (From Schummers *et al.* [19]).

Using moving oriented gratings, James Schummers *et al.* [19] have shown that

> "neurons near pinwheel centers have subthreshold responses to all stimulus orientations but spike responses to only a narrow range of orientations".

Far from a pinwheel (see figure 6), cells

> "show a strong membrane depolarization response only for a limited range of stimulus orientation, and this selectivity is reflected in their spike responses".

At a pinwheel center, on the contrary (see figure 7), only the spike response is selective. There is a strong depolarization of the membrane for all orientations.

This is an original solution to the problem of singularities, which is to have at the same time all orientations with a good orientation selectivity.

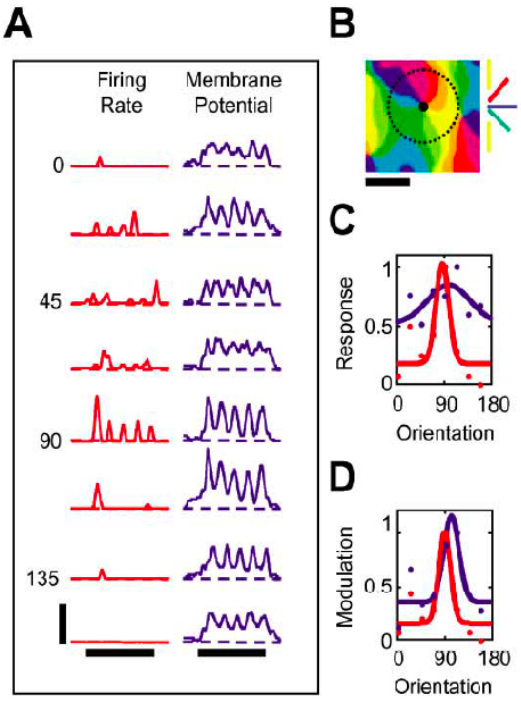

Figure 7: The response of a cell near a pinwheel center: spike response is selective to orientation while membrane depolarization is not. Scales: 3 spikes/s, 8mV, 2s. (From Schummers *et al.* [19]).

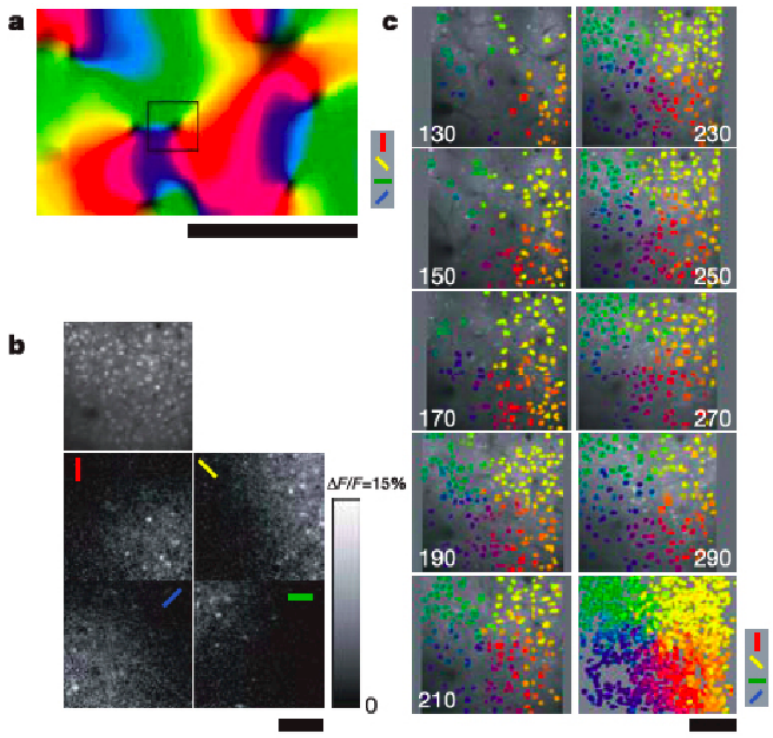

Figure 8: Pinwheels at single neuron resolution. (From Ohki [13]).

But the spatial and depth resolutions of optical imaging is not sufficient ($50\mu m$) and one needs *single neuron resolution* to understand the micro-structure of the pinwheels. It is now possible to observe it using two-photon calcium imaging in vivo (confocal biphotonic microscopy), which provides functional maps at single-cell resolution. Kenichi Ohki *et al.* [13] have shown that (in cat) pinwheels are higly ordered at the micro level and

> "thus pinwheels centres truly represent singularities in the cortical map".

Injection of calcium indicator dye (Oregon Green BAPTA-1 acetoxylmethyl esther) allows to label few thousands of neurons in a $300-600\mu m$ region. Then two-photon calcium imaging measures simultaneously calcium signals evoked by visual stimuli on hundreds of such neurons at different depths (from $130\mu m$ to $290\mu m$ by $20\mu m$ steps). (See figure 8).

> "This demonstrates the columnar structure of the orientation map at a very fine spatial scale".

It is a very interesting problem to imagine the possible structure of a connectivity implementing the sharp orientation tuning and the dendritic tree near the centre C (few tens μm) in an iso-orientation domain D. Ohki proposes some possibilities:

1. a dendritic tree biased towards D;
2. a dendritic tree symmetric, while the excitatory inputs are biased towards D;
3. a dendritic tree symmetric, excitatory inputs also symmetric but local and therefore inside D (good segregation near C);
4. a dendritic tree symmetric, excitatory inputs symmetric and uniformly integrated over a large dendritic area.

3.4 Other "engrafted" variables

Many other variables are "engrafted" in the pinwheel structure, which means that the fibration over R has fibers of dimension > 1. We must emphasize in particular the phase varying inside a single column, the ocular dominance, and the spatial frequency distributed along the rays of the pinwheels. Hübener *et al.* [9] have recorded the boundaries of the low spatial frequency domains. Statistically, the pinwheels are centered inside the frequency regions and the iso-orientation lines are strongly *transversal*, and even orthogonal, to the boundaries (see figure 9). So, after the dimensional collapse, independency between two "secondary" degrees of freedom is translated into a transversality condition.

3.5 The horizontal structure

The "vertical" retinotopic structure of the hypercolums and pinwheels is not sufficient for implementing a *global* coherence. To integrate local data into global structures, the visual system must be able to *compare* two retinotopically neighboring fibers P_a and P_b over two neighboring points a and b of the base R. This is a problem of *parallel transport*, which has been solved at the empirical level by the great discovery of "horizontal" cortico-cortical connections.

Cortico-cortical connections are slow ($\simeq 0.2$m/s) and weak and connect neurons of almost similar orientation in neighboring hypercolumns. This means that the V1 system is able to know, for b near a, if the orientation q at b is the same as the orientation p at a.

The next figure (10), due to William Bosking *et al.* [3], shows how a marker (biocytin) injected locally in a zone of specific orientation (green-blue) diffuses via horizontal cortico-cortical connections. The key fact is that the long range diffusion is highly anisotropic and restricted to

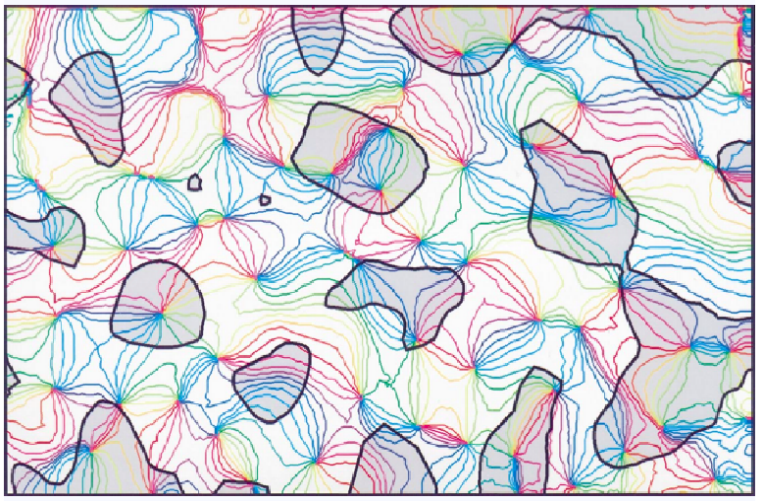

Figure 9: The transverse configuration between the orientation field and low spatial frequency domains. (From Hübener *et al.* [9]).

zones of the same orientation (the same color) as the initial one. Moreover, cortico-cortical connections connect neurons coding *aligned* pairs (a, p) and (b, q), that is pairs such that p and q are approximately the orientation of the axis ab.

> "The system of long-range horizontal connections can be summarized as preferentially linking neurons with co-oriented, co-axially aligned receptive fields". (Bosking *et al.* [3])

This experimental result is crucial since it shows that the well known Gestalt law of "good continuation" is neurally implemented.

In fact, a certain amount of *curvature* is allowed in alignements and we will come back to this important point.

3.6 Efficient coding and statistics of natural images

As resulting from an evolutionary process, RFs are adapted to a processing of natural images. As was emphasized by Joseph Atick [1], they seem to result from

> "efficiency of information representation".

An efficient coding must reduce redundancy and maximize the mutual information between visual input and neural response. Now, the statistic of natural images is very particular.

For instance the RFs of the ganglion cells of the retina and of the cells of the lateral geniculus nucleus decorrelate the selfcorrelation C of

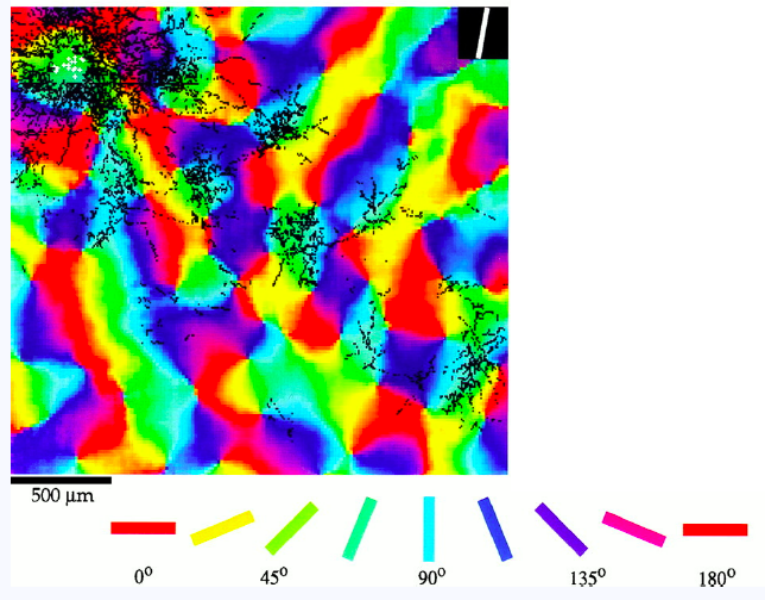

Figure 10: Diffusion of Biocytin along long-range horizontal connections. (From Bosking et al. [3]).

the signal I, $C(x - x') = \langle I(x).I(x')\rangle$.[1] According to Field's law, the power spectrum of C (its Fourier transform) is of the form $\widehat{C}(\omega) = \frac{1}{|\omega|^2}$ (ω is the frequency), which implies that it is scale invariant.

The functional architecture of V1 reflects the statistical properties of natural images concerning alignements and boundaries, i.e. "good continuation". The next figure (11), due to Mariano Sigman *et al.* [21] represents the correlation of orientations between two points O and a in the plane for $4,000$ natural images.

As Sigman explains:

> "Our findings provides an underlying statistical principle for the establishment of form and for the Gestalt idea of good continuation."
> "The geometry of the pattern of interactions in primary visual cortex parallels the interactions of oriented segments in natural scenes."

[1] Brackets $\langle\rangle$ symbolize mean values.

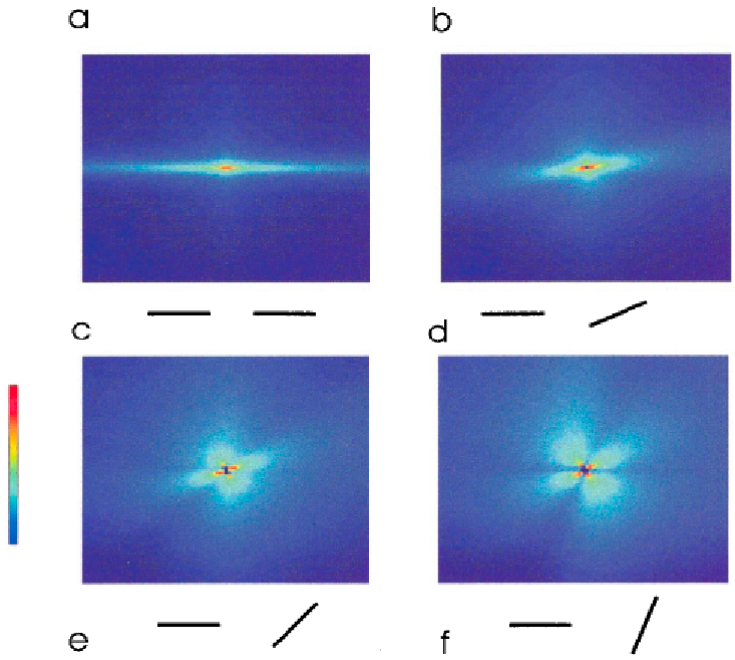

Figure 11: The correlation of orientations between two points O and a in the plane for $4,000$ natural images. (From Sigman et al. [21]).

4 Neurogeometry of V1

4.1 The contact structure of V1

We will now introduce natural mathematical models for these experimental results. We will begin with *idealized* models where pinwheels constitute a *continuous* field and come back in a second step to *discrete* more realistic models.

The first evidence is that the set $V = R \times P$ of contact elements (a, p) is coded by the simple neurons of V1. It is therefore natural to make the hypothesis that the functional architecture, that is the very specific connectivity of V1, implements a mathematical structure on V.

In fact, the experimental results we have presented mean essentially that the *fibration* $\pi : V = R \times P \to R$ and what is called in differential geometry the *contact structure* of π are neurally implemented. This fibration is essentially the space of 1-jets of curves C in R. If C is a smooth curve in R, it can be lifted to V. This lift Γ (called Legendrian) is the map $j : C \to V = R \times P$ wich associates to every point a of C the contact element (a, p_a) where p_a is the tangent of C at a. Γ, which represents C as the enveloppe of its tangents (projective duality), is the 1-jet of C.

4.2 Fonctionality of jet spaces

Jan Koenderink [10] strongly emphazised the importance of the concept of jet. Without jets, it is impossible to understand how the visual system could extract geometric features such as the tangent or the curvature of a curve:

> "geometrical features become multilocal objects, i.e. (...) the processor would have to look at different positions simultaneously, whereas in the case of jets it could establish a format that provides the information by addressing a single location. Routines accessing a single location may aptly be called points processors, those accessing multiple locations array processors. The difference is crucial in the sense that point processors need no geometrical expertise at all, whereas array processors do (e.g. they have to know the environment or neighbours of a given location)."

The key idea is therefore (as in Hamiltonian mechanics):

1. to add new independent variables describing local features such as orientation;

2. to introduce an integrability constraint enabling to integrate them into global structures.

Neurophysiologically, this boils down to add *feature detectors* and couple them via the functional architecture.

To every curve C in R is associated by lifting a Legendrian curve Γ in V. But the converse is of course completely false. Let (x, y, p) be coordinates in V. If $\Gamma = \{x, y(x),\ p(x)\}$ is a curve in V (transverse to the fibers of π), Γ is the lift of its projection $C = \{x, y(x)\}$ iff $p(x) = y'(x)$. This is an *integrability condition*: to represent a coherent curve in V, Γ must be an integral curve of the *contact structure* of the fibration π, which means that all the tangent vectors t of Γ must belong to the kernel of the differential 1-form $\omega = dy - pdx$. Indeed, $\omega = 0$ means simply that $p = dy/dx$. At each point $v = (a, p)$ of V, the kernel of ω is a *plane* K_v called the *contact plane* of V at $v = (a, p)$.

The vertical component p' of the tangent vector is then the *curvature* of C at a since $p = y'$ implies $p' = y''$.

4.3 Integrability condition and Association field

The integrability condition corresponds to the psychophysical experiments on what David Field, Anthony Hayes and Robert Hess [7] have called the *association field*. These authors explained experiments on

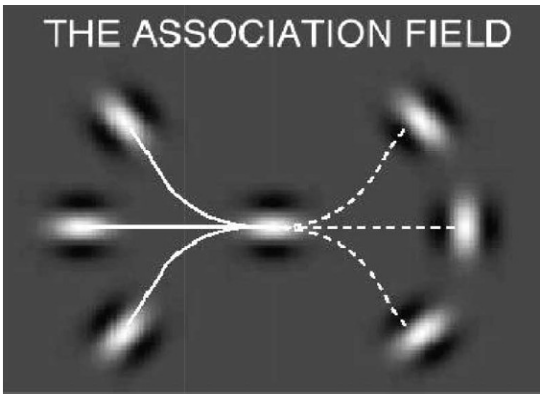

Figure 12: The Assocition Field according to Field, Hayes, and Hess [7].

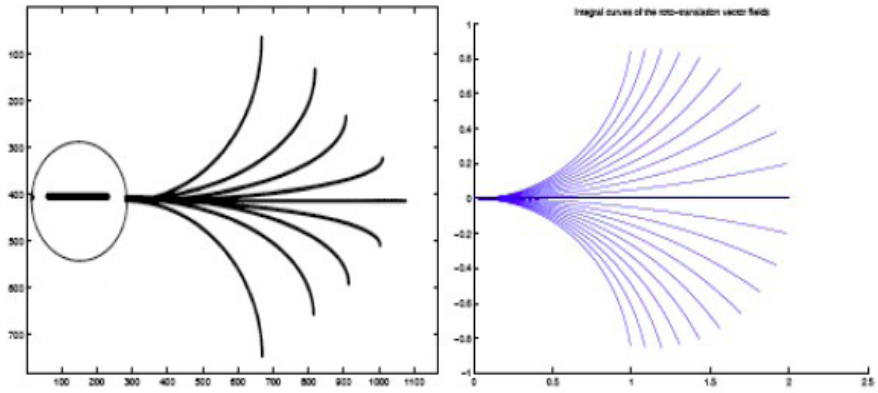

Figure 13: Left: the association field. Right: integral curves of the contact structure. (Graphics from A. Sarti).

good continuation by introducing a model of connectivity in V1 which is a discrete version of the integrability condition. In the next figures (12 and 13), the association field corresponds to the simplest integral curves of the contact distribution.

4.4 Contact structure and Heisenberg group

We will now recall some well known mathematical facts concerning the contact structure.

The first important mathematical fact is that the contact structure on V is *left-invariant* for a noncommutative *group* structure which is isomorphic to the Heisenberg group and is called the *polarized Heisenberg group*. The group law is given by the formula:

$$(x,y,p).(x',y',p') = (x+x', y+y'+px', p+p') \ .$$

If $t = (\xi, \eta, \pi)$ denotes any tangent vector of $\mathfrak{V} = T_0 V$, the tangent space of V at the neutral element $0 = (0,0,0)$, the Lie algebra $\mathfrak{V}$ has the Lie bracket

$$[t,t'] = [(\xi,\eta,\pi),(\xi',\eta',\pi')] = (0, \xi'\pi - \xi\pi', 0) \ .$$

$\mathfrak{V}$ is generated by the 3 vectors $\{t_1 = \partial_x + p\partial_y, t_2 = \partial_p, -t_3 = \partial_y\}$ (tangent vectors are interpreted as oriented derivatives) satisfying the basic noncommutative relation $[t_1, t_2] = t_3$, the other brackets being $= 0$. The 2 vectors $\{t_1 = \partial_x + p\partial_y, t_2 = \partial_p\}$ span the contact plane K_v at $v \in V$.

4.5 Contact structure and Euclidean group

With Alessandro Sarti and Giovanna Citti [18] we emphasized the fact that it is more natural to work without any privileged x-axis, that is in the fibration $\pi : V = R \times P \to R$ with $P = \mathbb{S}^1$ and with the contact form $\omega = -\sin(\theta)dx + \cos(\theta)dy$, that is $\cos(\theta)(dy - pdx)$.

The contact planes are now spanned by $\{X_1, X_2\}$ with $X_1 = \cos(\theta)\,\partial_x + \sin(\theta)\,\partial_y$ and $X_2 = \partial_\theta$ with Lie bracket $[X_1, X_2] = \sin(\theta)\,\partial_x - \cos(\theta)\,\partial_y = -X_3$. But, contrary to the polarized Heisenberg group case, all the other brackets don't vanish. We have $[X_1, X_3] = 0$, but $[X_2, X_3] = X_1$, the "Reeb" vector X_3 being the characteristic vector orthogonal to K_v defining a scale through the relation:

$$\omega(X_3) = (-\sin(\theta)\,dx + \cos(\theta)\,dy)(X_3) = \sin^2(\theta) + \cos^2(\theta) = 1 \ .$$

5 Models for pinwheels

So far, we have presented experimental data and an idealized mathematical model for them. The problem is now to make the link with concrete realistic models of pinwheels. The main difficulty is to introduce good hypotheses on the behavior of orientation selectivity at the singularities.

5.1 Wolf-Geisel's model

The field of preferred orientations $\vartheta(a) = e^{i\theta(a)}$ of simple neurons of V1 can be described as a section of the fibration $\pi : R \times P \to P$ defined outside the lattice L of the centers of the pinwheels. Fred Wolf and Theo Geisel [22] have proposed models of this type for the learning of the orientation selectivity. They model hypercolumns by a continuous *complex field* $z(a) = \rho(a)e^{i\theta(a)}$ where the spatial phase $\theta(a)$ codes the orientation preference and the module $\rho(a) = |z(a)|$ the selectivity strength. The complex value z represents therefore a section of the fibration with base

R and fiber $\mathbb{C}$ and the singular points (centers of pinwheels) correspond to *zeroes* of z.

The morphogenesis of the field z can be described by a PDE of the form $\frac{\partial z(a,t)}{\partial t} = F\left(z(a,t)\right) + \eta\left(a,t\right)$, where F is a nonlinear operator and η a stochastic term. Such dynamics can be induced by Hebbian learning processes, $F\left(z(a)\right)$ being the mean of $z(a)$ for stimuli changing rapidly according to a given law of probability.

A problem with this interesting model is that, due to the continuity of z, $|z(a)|$ is very small near the centers of the pinwheels and the orientation selectivity is therefore very weak. When the limit of the mesh of the lattice $L \to 0$, z has to vanish everywhere. But experimental data are not completely compatible with such a model since there exists a good orientation selectivity at the singular points.

5.2 Blowing-up and nonstandard models

Another class of models make precisely the hypothesis that all orientations must be present with a good selectivity at the singularities. But then, how can one model the dimensional collapse of the 3D abstract space $V = \mathbb{R}^2 \times \mathbb{P}^1$ onto 2D neural layers?

5.2.1 Blowing-up

An idea could be to use the concept of "blowing-up". In algebraic geometry, the *blowing-up* of a point $0 = (0,0)$ in the plane $M = \mathbb{R}^2$ associates to every point $a = (x,y) \neq (0,0)$ of M the line $0a$. One gets the map

$$\begin{aligned} \delta : \mathbb{R}^2 - \{0\} &\to \mathbb{P}^1 \\ a = (x,y) &\mapsto \delta(a) = p = \tfrac{y}{x} \end{aligned}$$

The graph of δ is a helicoidal ruled surface H in $V = \mathbb{R}^2 \times \mathbb{P}^1$ which is isomorphic to $\mathbb{R}^2 - \{0\}$ through the projection π. Its closure $\overline{H}$ is a helicoid with an exceptional fiber $\pi^{-1}(0) = \Delta \simeq \mathbb{P}^1$. If d is a straight line in $\mathbb{R}^2$, the closure d' of the inverse image of $\pi^{-1}(d - \{0\})$ is the set of points $(\lambda a, \delta(a) = p)$ of $V = \mathbb{R}^2 \times \mathbb{P}^1$, that is the line d at height $\delta(a) = p = \frac{y}{x}$. When d rotates in the plane $\mathbb{R}^2$, d' rotates above $\mathbb{R}^2$ and translates along Δ.

As the inverse image of 0 by π is $\Delta = \mathbb{P}^1$, the blowing-up is in some sense of "intermediary" dimension between $2D$ and $3D$. It is an unfolding of a $2D$ orientation wheel along a third dimension.

This construction can be understood as an interpretation of *polar coordinates* in terms of the fibration $\pi_1 : \mathbb{R}^2 \times \mathbb{S}^1 \to \mathbb{R}^2$. Indeed, in the plane $\mathbb{R}^2 - \{0\}$, the argument $\theta_1(a) \in [0, 2\pi]$ of a point a is well defined and one can therefore consider the section ϑ_1 of π_1 defined by $\vartheta_1 : a \to \vartheta_1(a) = \left(a, e^{i\theta_1(a)}\right)$. The fibration $\pi : \mathbb{R}^2 \times \mathbb{P}^1 \to \mathbb{R}^2$ is the quotient of the fibration $\pi_1 : \mathbb{R}^2 \times \mathbb{S}^1 \to \mathbb{R}^2$ through the identification of

θ_1 with $\theta_1 + \pi$ (that is of $e^{i\theta_1}$ with $-e^{i\theta_1}$) and ϑ_1 lifts into π_1 the section of π defined by $\vartheta : a \to \vartheta(a) = \left(a, e^{i\theta(a)}\right)$ where $\theta(a) = \theta_1(a)/2 \in [0, \pi]$ is now considered modulo π. $\vartheta_1(a)$ is constant along the rays $\theta = \text{cst}$ and, when it is lifted from $\mathbb{R}^2 \times \mathbb{P}^1$ into $\mathbb{R}^2 \times \mathbb{S}^1$, the surface H becomes the image of ϑ_1.

5.2.2 Infinitesimal blowing-up

In a second step, one can localize the blowing-up model of a pinwheel and restrict it to neighborhoods U of 0. One can then take the germ, that is the limit w.r.t the filter of neighborhoods. In the germ, $p = \frac{dy}{dx}$ is in the kernel of the differential 1-form $\omega = dy - pdx$. Completing the $\mathbb{R}$-fiber as a $\mathbb{P}^1$-fiber Δ, one gets a model for a single pinwheel.

5.2.3 Parallel infinitesimal blowing-up

In a third step, one can blow-up in parallel several points a_i of a lattice L and glue the local pinwheels (a_i, Δ_i) using a field induced by endowing the a_i with topological charges (chirality). One gets that way a model for a lattice L of pinwheels.

The problem is now to understand how this *discrete* blowing-up model of pinwheels can yield the continuous model of the functional architecture as a contact structure. For that, we have to achieve two opposite constructions. First, to recover the fibration π when the mesh of $L \to 0$. Second, to interpret the dimensional collapse, that is the possibility of pulling down the fibers Δ_i into neighborhoods of the points a_i.

5.2.4 Nonstandard pinwheels

So, in a fourth step, we consider lattices of points a_i with a mesh $\to 0$. The idea is that one could recover the fibration $\pi : \mathbb{R}^2 \times \mathbb{P}^1 \to \mathbb{R}^2$ endowed with its contact structure by blowing-up in parallel *all* the points of the plane $\mathbb{R}^2$.

Using nonstandard analysis (in the sense of Robinson and Luxemburg), one can restrict the infinitesimal blowing-up to the monads $\mu(a) = \{(x + dx, y + dy)\}$ of the standard points $a = (x, y)$ of $\mathbb{R}^2$. When one blows-up the standard point a in its monad (which is an external set), one gets an exceptional fiber Δ^* whose standard points correspond to standard $p = dy/dx$.

In such a model, Hubel's method of "engrafting" secondary variables by pulling down the fibers Δ^* into neighborhoods of the points a would consist in "compactifying" (as in the Kaluza-Klein models in physics) the fiber Δ^* over a and including it in the external set $\mu(a)$.

If one uses general infinitesimals, dy/dx will be a nonstandard real p^* and we will have $p = \text{st}(p^*)$. It is not easy to reformulate differential forms in this context. But one can also choose an infinitesimal of ref-

erence ε and consider the disc D of center a and radius ε in $\mu(a)$. The exceptional fiber Δ^* can then be identified with the boundary ∂D. If the infinitesimal increments da are chosen on ∂D, that is if $dx = \varepsilon X$ and $dy = \varepsilon Y$ with X, Y standard, then $dy/dx = Y/X = p$ is standard. If D^n is the disc of radius ε^n, $D - D^{n+1}$ corresponds to the n-jets of germs of functions at a.

6 Conclusion

We have seen what type of geometrical models are adequate for modelling pinwheels and understanding at a very deep level how the brain can do geometry. The key mathematical structure is a contact structure of abstract dimension 3 and the key material fact is that this 3D structure is discretized and implemented in a 2D cortical layer. We introduced a blowing-up model for pinwheels and show, using a nonstandard perspective, how the continuous limit retrieves the contact structure.

It would be interesting to work out a "constructive" version of this nonstandard model in the framework of "discrete geometry" in the sense of Wallet and Harthong-Reeb. It could be a better model for pinwheels as a discretization of the contact structure.

7 Addendum

After the beautiful Conference *Des Nombres et des Mondes* held in June 2011, I had the opportunity of reading the interesting correspondance between Pierre Deligne, Bernard Malgrange, and Jean-Pierre Ramis on "Irregular singularities" published by the Société Mathématique de France. In a letter of the 7th of January 1986 concerning singularities of analytic functions and Gevrey classes, P. Deligne [5] introduced the concept of a "fat point". The idea is to substitute for a point $a \in \mathbb{C}$, say $a = 0$, a small disk D with boundary Δ and to consider the space $\widetilde{\mathbb{C}} = \mathbb{C}^* \cup D$ with the topology of the real blowing-up on $\mathbb{C}^* \cup \Delta$.

Having the opportunity of coming back to La Rochelle in December 2011, I told Guy Wallet about this construction and Guy told me that they discussed it a long time ago in his lab with Michel Berthier. Michel brought to my attention the text of Jean-Pierre Ramis [17] on the last work of Jean Martinet [12] on Gevrey classes, where Martinet used such a construction with infinitesimal disks D in the sense of Nonstandard Analysis.

It would be perhaps interesting to try to construct models of pinwheels where the lattice L of pinwheels would be a lattice of infinitesimal fat points in the sense of Deligne-Martinet. Such models would be intermediary between Wolf-Seigel's models and 1-jet fiber bundles models.

References

[1] Atick, J. Could Information theory provide an ecological theory of sensory processing?, *Network*, 3 (1992) 213-251.

[2] Baxter, W.T., Dow B.M. Horizontal organization of orientation-sensitive cells in primate visual cortex, *Biological Cybernetics*, 61, 3 (1989) 171-182.

[3] Bosking, W.H., Zhang, Y., Schoenfield, B., Fitzpatrick, D. Orientation Selectivity and the Arrangement of Horizontal Connections in Tree Shrew Striate Cortex, *Journal of Neuroscience*, 17, 6 (1997) 2112-2127.

[4] Citti, G., Sarti, A. A cortical based model of perceptual completion in the roto-translation space, *Journal of Mathematical Imaging and Vision*, 24, 3 (2006) 307-326.

[5] Deligne, P., Malgrange, B., Ramis, J-P. *Singularités irrégulières. Correspondance et documents*, Société Mathématique de France, 2007.

[6] Field, D.J. Relations between the statistics of natural images and the response properties of cortical cells, *Journal of the Optical Society of America*, A, 4, 12 (1987) 2379-2394.

[7] Field, D.J., Hayes, A., Hess, R.F. Contour integration by the human visual system: evidence for a local "association field", *Vision Research*, 33, 2 (1993) 173-193.

[8] Hubel, D.H., *Eye, Brain and Vision*, Scientific American Library, W.H. Freeman & Co, New York, 1988.

[9] Hübener, M., Shoham, D., Grinvald, A., Bonhöffer, T. Spatial relationships among three columnar systems in cat area 17, *Journal of Neurosciences*, 17 (1997) 9270-84.

[10] Koenderink, J.J., Van Doorn, A.J. Representation of local geometry in the visual system, *Biological Cybernetics*, 55 (1987) 367-375.

[11] Maldonado, P. E., Gödecke, I., Gray, C. M., Bonhöffer, T. Orientation Selectivity in Pinwheel Centers in Cat Striate Cortex, *Science*, 276 (1997) 1551-1555.

[12] Martinet, J. Introduction à la théorie de Cauchy sauvage (unpublished). See Ramis [17].

[13] Ohki, K., Chung, S., Kara, P., Hübener, M., Bonhöffer, T., Reid, R.C. Highly ordered arrangement of single neurons in orientation pinwheels, *Nature*, 442 (2006) 925-928.

[14] Petitot, J. Rappels sur l'Analyse non standard, *La Mathématique non standard* (J-M. Salanskis, H. Barreau, eds.), Editions du CNRS, Paris, 1989, 187-209.

[15] Petitot, J. The Neurogeometry of Pinwheels as a Sub-Riemannian Contact Structure, *Neurogeometry and Visual Perception* (J. Peti-

tot, J. Lorenceau, eds.), *Journal of Physiology-Paris*, 97, 2-3 (2003) 265-309.

[16] Petitot, J. *Neurogéométrie de la vision. Modèles mathématiques et physiques des architectures fonctionnelles*, Les Editions de l'Ecole Polytechnique, Distribution Ellipses, Paris, 2008.

[17] Ramis, J-P. Les derniers travaux de Jean Martinet, *Annales de l'Institut Fourier*, 42, 1-2 (1992) 15-47.

[18] Sarti, A., Citti, G., Petitot, J. On the Symplectic Structure of the Primary Visual Cortex, *Biological Cybernetics*, 2006, 98, 1 (2008) 33-48.

[19] Schummers, J., Marino, J., Sur, M. Synaptic integration by V1 neurons depends on location within the orientation map, *Neuron*, 36 (2002) 969-978.

[20] Shmuel, A., Grinvald, A. Coexistence of linear zones and pinwheels within orientation maps in cat visual cortex, *PNAS*, 97, 10 (2000) 5568–5573.

[21] Sigman, M., Cecchi, G.A., Gilbert, C.D., Magnasco, M.O. On a common circle: Natural scenes and gestalt rules, *PNAS*, 98, 4 (2001) 1935-1940.

[22] Wolf, F., Geisel, T. Spontaneous pinwheel annihilation during visual development, *Nature*, 395 (1998) 73-78.

[23] Young, R.A., Lesperance, R.M., Meyer, W.W. The Gaussian Derivative model for spatio-temporal vision, *Spatial Vision*, 14, 3-4 (2001) 261-319.